SINERGI Vol. 26, No. 2, June 2022: 155-164
http://publikasi.mercubuana.ac.id/index.php/sinergi
http://doi.org/10.22441/sinergi.2022.2.004

Seismic performance of moment frames under multiple fling-step pulse ground motions

Ade Faisal[1*], Afiful Anshari[1], Bambang Hadibroto[2], Ahmad Fahmy Kamarudin[3]
[1]Department of Civil Engineering, Faculty of Engineering, Universitas Muhammadiyah Sumatera Utara, Indonesia
[2]Department of Civil Engineering, Faculty of Engineering, Universitas Negeri Medan, Indonesia
[3]Faculty of Civil Engineering and Environment, Universiti Tun Hussein Onn Malaysia, Malaysia

Abstract
The displacement fling-step pulse seldom signatures near-field earthquake in its ground motions. It is well recognized that the near-field ground motion with velocity pulse amplifies the building drift larger than the regular ground motion. Recent findings explain that the building experiences minor damage to collapse is not caused only by the single earthquakes, which in many cases are due to repeated ground motion. The seismic performance of moment frames under the displacement fling-step pulse motion is not studied, particularly when this type of motion applies. Thousands of nonlinear inelastic response history analyses are conducted in order to find out the inter-story drifts, as the engineering demand parameter throughout the incremental dynamic analysis, on the 5 to 20-story moment resisting frames under the influence of multiple ground motions with a fling-step pulse. The special, intermediate, and ordinary types of moment frames are considered, respectively. On average, the evaluation result explains that the intensity measure of multiple ground motions with a fling-step pulse needs 68.37% lower than the single ground motion in order to produce the near collapse inter-story drift. This means the multiple ground motion with fling step pulse increases the probability of near collapse of frames significantly.

Keywords:
Engineering demand parameter;
Near collapse inter-story drift;
Incremental dynamic analysis;
Intensity measure;
Probabilistic analysis;

Article History:
Received: June 30, 2021
Revised: November 16, 2021
Accepted: December 9, 2021
Published: June 1, 2022

Corresponding Author:
Ade Faisal
Department of Civil Engineering,
Faculty of Engineering,
Universitas Muhammadiyah
Sumatera Utara, Indonesia
Email: adefaisal@umsu.ac.id

INTRODUCTION

Many studies have explained that the near-field ground motion with velocity pulse significantly affects multi-story reinforced concrete (RC) frames, building with either regular or irregular plans [1, 2, 3]. By conducting the incremental dynamic and probabilistic analysis, Dahal et al., [2] discussed the collapse risk of the RC frame affected by the velocity pulse content in ground motion.

However, they have not specifically explained the effect of fling-step pulse on the moment resisting frame (MRF). The fling-step pulse in ground motion is indicated by a one-sided long-period pulse in its velocity time history and creates a permanent static drift in its displacement time history [4].

The previous studies have clearly indicated that the extensive damage to the structures might be occurred due to the sequence of earthquakes. Mohsenian et al. [4] have investigated the damage to 6 types of RC and steel structures under a sequence of earthquakes. Di Trapani and Malavisi [5] identified the probability of collapse and its risk of damage for RC frames underground motion sequences. These recent studies have found that the multiple earthquakes caused the damage extended significantly in comparison with the single earthquake effect.

The reinforced concrete (RC) structures affected by the multiple ground motion have been studied by Guo et al. [6] to identify the coupling mechanism between incremental seismic damage (ISD) and recorded maximum response, the periods' transition, and the characteristics of multiple ground motion. They found that mainshocks were not consistently causing the occurrence of ISD.

Moreover, multiple near-field earthquakes also propagate larger drift than a single earthquake's effect. Oyguc et al. [7] has found that the drift increased up to 35% on the RC buildings. They used the real building and previous experimental buildings as the RC model. They noticed that the element's damage could not be captured on higher modes. Di Sarno and Plugliese [8] introduced the effect of various levels of corrosion on the RC structures' vulnerability under multiple seismic motions. The consistent angle of the incident on the frame was found could could feature prominently in the drift of of 3-, 9-, and 20-story steel MRF under 2D and 3D modelling approaches [9].

Recently, the different study on the stiffness irregularity of 3-, 6-, and 9- story steel MRF under the effect of mainshock-aftershock sequences has demonstrated that the aftershock effect could have a larger effect than the mainshock [10, 11]. The study found that the mainshock-aftershock motion significantly caused the effect on the drift if the height-wise variation was considered. It was declared that the occurred soft storey has increased the inter-story drift located at the modified and neighboring stories, and thus it has decreased at other stories.

The corresponding change in the angle of incidence of multiple ground motions can significantly influence the response of the single degree of freedom system [8][12].

Unfortunately, the effect of multiple earthquakes containing displacement fling-step pulse on the MRF was not been fully investigated yet, since the available records were scarce. Therefore, the goal of this study is to investigate the seismic response of MRF affected by multiple ground motions containing the fling-step effect based on the available ground motion records from the 1994 Northridge, 1999 Chi-Chi, and 1999 Kocaeli earthquakes.

METHOD

RC Frame Model

The archetype of MRF consisted of 5-, 10-, 15- and 20-story with the regular floor plan shape, masses and stiffness are evaluated. The MRFs are built above the soft soil in Banda Aceh City, Indonesia.

The special moment resisting frame (SMF) type is used, which is commonly built with R = 8 for a RC frame. Moreover, the intermediate (IMF) and ordinary moment resisting frame (OMF) (with R = 5 and 3 are assumed to be built on the medium and hard soil type, respectively, in the same city) are also considered in the study. Figure 1 depicted the plan view and the 2-dimensional frame sections of the structural model. The length of all beams is 6.0 m, and the height of all columns is 3.5 m (except for columns on the ground floor which are 4.5 m in height). The study has considered the concrete and rebar yield strengths for all models, which are f'_c 40 MPa and f_y 400 MPa, respectively. The model's natural period is set to be 0.41 s, 0.80 s, 1.16 s, and 1.58 s for 5-, 10-, 15-story, and 20-story RC frames, respectively. Since this study is related to the seismic assessment of existing designed MRF, almost all of the methods in the following sections are based on FEMA P-58 and its associated supporting documents and references [13][14].

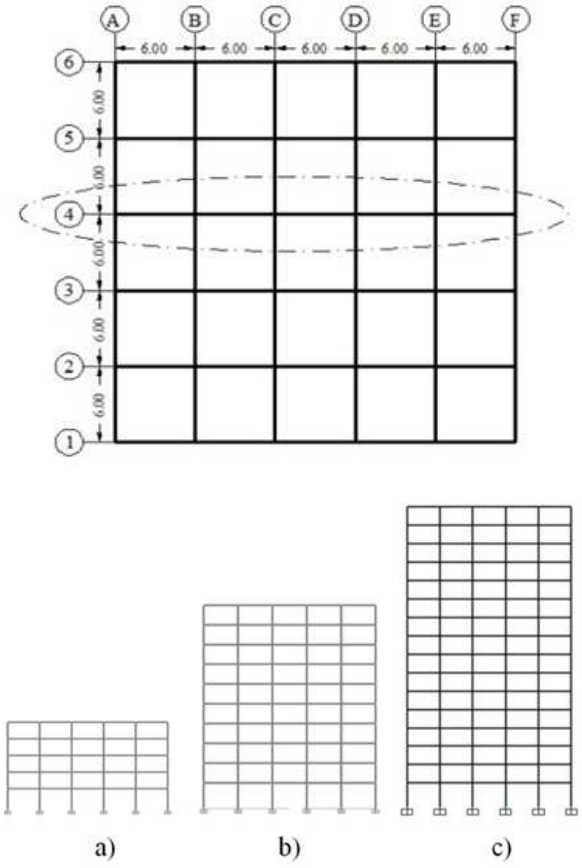

Figure 1. Models' Plan View and Its 2-Dimensional Frame Section of 5-, 10-, and 15-Story

Material Model

To model the nonlinearity and inelasticity of material, we follow the famous generic frame method, also well-known as the FEMA method, instead of using the concrete section analysis for the element strength and deformation capacity. The flexural forces sourced from elastic designed result are used as the yield flexural strength (M_y) of an element. Its maximum force is based on the empirical value of 1.13 M_y. The strong column weak beam mechanism is then adjusted accordingly based on these elements' flexural forces to fulfil the code requirements. The Modified-Takeda hysteresis rules are employed [1][3] to control the material nonlinearity and inelasticity during cycle loads, as shown in Figure 2. The unloading and reloading parameters, α = 0.3 and β = 0.6, respectively, are used for reinforced concrete beam and column members, which are based on some experimental works.

Elements Model

The ductile system's collapse capacity, such as the SMF of the RC system, is mostly affected by the plastic rotation capacity θ_p, which is mainly controlled by the onset of rebar buckling or the concrete core's loss of confinement. One of the options for evaluating the MRF in FEMA P-58 [14][15] is through the rotation capacity based on evaluating and calibrating the database of RC columns from previous experimental testing. This current study uses this rotation capacity of RC beam-column member, namely θ_p = 0.04 rad for SMF, whereas IMF and OMF employ θ_p = 0.02 rad. The ratio of M_y with elastic rotation stiffness (K_0 = 6EI/L) of the member was taken to define the yield rotation of the member θ_y.

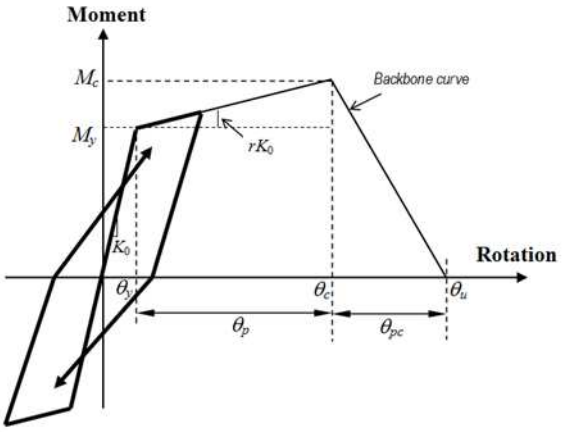

Figure 2. Modified-Takeda hysteresis and backbone curve in lumped plasticity model of nonlinear inelastic elements [1]

The post-yield stiffness ratio or bi-factor (r) of the member's hysteresis rule was estimated based on the ratio of capping moment and yield moment M_c/M_y and the ductility of plastic rotation capacity ($\mu_{\theta,c}$) which is defined as follows:

$$r = \frac{M_c - M_y}{K_0(\mu_{\theta,c} - 1)\theta_y} \quad (1)$$

where

$$\mu_{\theta,c} = \frac{\theta_c}{\theta_y} = \frac{\theta_y + \theta_p}{\theta_y} \quad (2)$$

$$\theta_y = M_y / K_0 \quad (3)$$

This study selects the post capping rotation of θ_p = 0.06, M_c/M_y =1.13, and assumes M_c is equal to maximum moment (M_{max}) since the ratio of M_c/M_y reflects the capacity of member in strength hardening as well.

Strength Degradation

The strength degradation of the member up to residual strength of 1% of initial strength (yield moment) at the ultimate rotation ductility, $\mu_{\theta,u}$ is considered in this study. At 1% of initial strength, the strength is sufficiently very low to represent strength in a collapsed state [16]. The capping rotation ductility, $\mu_{\theta,c}$, is defined through (4); whereas ultimate rotation ductility, $\mu_{\theta,c}$, is obtained based on yield rotation (θ_y), capacity of plastic rotation (θ_c), and capacity of post-capping rotation (θ_{pc}), as follows:

$$\mu_{\theta,u} = \frac{\theta_u}{\theta_y} = \frac{\theta_y + \theta_p + \theta_{pc}}{\theta_y} \quad (4)$$

Ground Motions and Intensity Measure

In a previous study, the as-recorded mainshock-aftershock and repeated artificial earthquakes were used extensively in the seismic evaluation of the buildings. They were not considered the pulse type content in their ground motions. This type of ground motion could not be employed in this study. It was because this study intended to assess the seismic performance of RC structure affect by repeated earthquakes containing fling-step only. Since the ground motion records with fling-step were rarely available, this study used some records from the 1999 Chi-Chi, 1999 Kocaeli, and 1994 Northridge earthquakes. To develop these artificial sequences motions, the record from the *Pacific Earthquake Engineering Research* (PEER) *Next Generation Attenuation* (NGA) were selected, as listed in Table 1.

Table 1. The selected records of ground motion containing fling-step pulse effect sourced from PEER NGA and COSMOS

Record No	Earthquake	M_W	Station	Dist. (km)	Site Class	Comp.	PGA (g)	PGV (cm/s)	PGD (cm)
1	Chi-Chi	7.6	TCU052	1.8	D	EW	0.35	178.00	493.52
2	Chi-Chi	7.6	TCU068	3.0	D	EW	0.50	277.56	715.82
3	Chi-Chi	7.6	TCU074	13.8	D	EW	0.59	68.90	193.22
4	Chi-Chi	7.6	TCU084	11.4	C	EW	0.98	140.43	204.59
5	Chi-Chi	7.6	TCU129	2.2	D	EW	0.98	66.92	126.13
6	Kocaeli	7.4	Yarimca	3.3	D	EW	0.23	88.83	184.84
7	Kocaeli	7.4	Izmit	4.3	B	EW	0.23	48.87	95.49
8	Chi-Chi	7.6	TCU102	1.2	D	EW	0.29	84.52	153.88
9	Chi-Chi	7.6	TCU089	8.3	C	EW	0.34	44.43	193.90
10	Chi-Chi	7.6	TCU049	3.3	D	EW	0.27	54.79	121.77
11	Chi-Chi	7.6	TCU067	1.1	D	EW	0.48	94.31	181.25
12	Chi-Chi	7.6	TCU075	3.4	D	EW	0.32	111.79	164.36
13	Chi-Chi	7.6	TCU076	3.2	D	EW	0.33	65.93	101.65
14	Chi-Chi	7.6	TCU072	7.9	D	EW	0.46	83.60	209.67
15	Chi-Chi	7.6	TCU065	2.5	D	EW	0.76	128.32	228.41
16	Chi-Chi	7.6	TCU078	8.3	D	EW	0.43	41.88	121.23
17	Chi-Chi	7.6	TCU082	4.5	D	EW	0.22	50.49	142.78
18	Chi-Chi	7.6	TCU128	9.1	C	EW	0.14	59.42	91.05
19	Chi-Chi	7.6	TCU071	4.9	D	NS	0.63	79.11	244.05
20	Northridge-01	6.7	LA-Sepulveda	6.7	C	4C	0.46	13.80	26.13

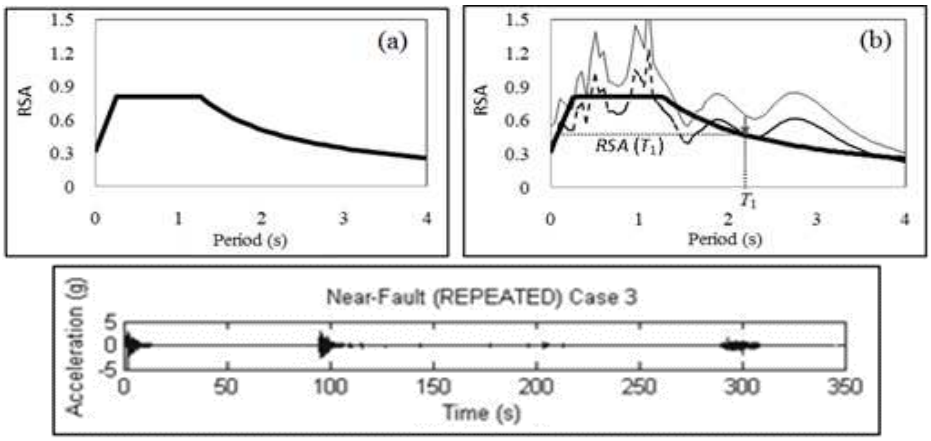

(c)

Figure 3. Example of Multiple Ground Motions' Model: a) Elastic Design Spectra for Banda Aceh City, b) Illustration of Scaling Process of Ground Motion, (c) Example of 3 Times Multiple Ground Motions

The fault mechanism, distance of source-to-site (≤ 15 km), magnitude, and soil type are employed as the selection criteria of ground motion records. The selected ground motion records contain near-field fling-step pulse effects. The elastic designed spectrum acceleration at the fundamental period of models, RSA(T_1), was referred for the method of ground motion modification. This parameter was also employed as the the intensity measure (IM) in this study (see Figure 3). In Figure 3a, the designed spectrum response acceleration for Banda Aceh City is depicted, which was developed based on based on the Indonesian seismic code, SNI 1726:2012 [18]. This Indonesian code was originally adopted from standard ASCE/SEI 7-10 [19].

The zero motions with 50 seconds of duration were inserted after randomly pairing the modified ground motion to simulate the multiple ground motions (Figure 3). It was done to allow the structure to pose the free vibration before starting the next ground motion. The study used two times and three times multiple ground motions to be induced on the MRF models in performing the incremental dynamic analysis. The seismic performance results in the form of inter-story drift (*EDP*), as well as *RSA*(T_1), as of intensity measure (*IM*) for specific (*EDP*), were then compared with EDP caused by the single ground motion having fling-step pulse-type.

Structural Analysis and Collapse Limit State

The Indonesian Standard SNI 1726-2012 [17] and ASCE/SEI 7-10 [18] were employed for the elastic design phase of the 2-dimensional RC frames. The designed flexural forces of 5-, 10-, 15-, and 20-story RC frames were defined based

on the response spectrum method. The nonlinear response history analysis with lumped plasticity model was conducted to define the near collapse state of the system and IM of motions using Ruaumoko 2D v.4.0 as the tool [16]. This analysis was done according to the seismic performance assessment guideline as conditioned in FEMA P-58 [14, 15, 16].

The near collapse inter-story drift (*IDR* = 2%) state is the engineering demand parameter (*EDP*), which is identified through the incremental dynamic analysis (IDA). In IDA, the *IM* = *RSA*(T_1) is repeatedly scaled to get the level of IM at which each ground motion causes *EDP*'s failure criterion, such as near collapse or collapse drift. Thus, a dataset of IM corresponding to the near collapse, namely *RSA*(T_1), is obtained through a linear interpolation and subsequently assumed as lognormal distributed for the specific *EDP* state. From IDA, the following parameters, namely, μ and β, median and standard deviation, respectively, are defined by fitting the interpolated *IM* through the method of moments as follows:

$$\log[\mu_{RSA(T_1)}] = \frac{1}{n}\sum_{i=1}^{n}\log[RSA(T_1)]_i \quad (5)$$

$$\beta_{\log[RSA(T_1)]} = \sqrt{\frac{\sum_{i=1}^{N}(\log[RSA(T_1)] - \log[\mu_{RSA(T_1)}])^2}{N-1}} \quad (6)$$

In order to develop the probability function for specific near collapse EDP, as discussed in the next section, this dataset was then fed to the fragility function.

Fragility function for Near Collapse

The fragility function was commonly used to express the probability function of any limited state of interest. In this study, the 5% damping response spectrum acceleration at the considered structures' period was employed as the IM. This IM resulted from nonlinear dynamic structural analysis and was then executed using statistical procedures to develop the probability function. Combining this fragility function with a ground motion hazard function could predict the mean annual rate of near structural collapse. A lognormal cumulative distribution function was commonly employed to develop the fragility function, as follows:

$$P[EDP \geq IDR_{\max} \mid R = RSA(T_1)] = \Phi\left(\frac{\log\left(RSA(T_1)/\mu_{RSA(T_1)}\right)}{\sqrt{\beta^2_{\log[RSA(T_1)]} + \beta^2_u}}\right) \quad (7)$$

Where P [$EDP \geq IDR_{\max}$; R = *RSA*(T_1)] is the probability of reaching or exceeding near collapse state *EDP* (so-called probability of near collapse) while a ground motion induces the structure with *RSA*(T_1); $\Phi(.)$ is the function of standard lognormal cumulative distribution; μ*RSA*(T_1) is the median of *IM* that would cause near collapse; and $\beta_{\log}$[*RSA*(T_1)] is the standard deviation of the *IM* that would cause near collapse *EDP*, in the form of maximum inter-story drift ratio, $IDR_{\max}$.

The IDA's result was not all the time could reach the targeted limit state of collapse in developing the fragility function. Baker [20] has developed a procedure to fix the dataset to predict the fragility function. The study also adopts the recommendation of FEMA P-58 guidelines to permanently increase the logarithmic standard deviation (by adding β_u = 0.1). It is done so since the uncertainty in the analytically-based fragility curve could not adequately and accurately represent the true variability [21] [22]

RESULTS AND DISCUSSION

In the incremental dynamic analysis (IDA) and collapse probability function, the employed structural model and its ground motion and the number dataset to be tested played an important role. In this section, the IDA result is presented based on the median value of maximum inter-story drift ($IDR_{\max}$), selected as the engineering demand parameter (EDP), and the median value of intensity measure *IM* = *RSA*(T_1). Moreover, global elastic stiffness and global post-elastic stiffness are discussed as well. The global elastic stiffness is represented by initial linear lines in the IDA curve, whereas after-turning-point lines represent the global inelastic stiffness. The changes in the direction of these lines are caused by the occurrence of plastic hinges in the element of structures due to the decrement of *IM*. The median IDA curves for the MRF with 5-, 10-, 15 and 20-story induced by a single and repeated 2x and 3x earthquakes were depicted in Figure 4 and Figure 5. These earthquakes were considered as 1GM, 2GM, and 3GM, respectively. For concise and simplicity, the next paragraphs use *IM* and EDP to explain *RSA*(T_1) and near collapse *IDR*, respectively.

The probabilistic analysis in this study produced the standard deviation of *IM* β_{IM} = 0.16 to 0.33 for all considered MRF. Porter et al. [20] found that commonly β_{IM} = 0.2 to 0.6, after including the uncertainty factor β_u, whereas others explained that commonly β = 0.4 was used to develop the fragility function without uncertainty factor [20]. Basone et al. [21] indicated their dataset achieving β = 0.29 to 0.60

when assessing the seismic fragility curve of RC buildings with T_1 =0.34 s. They evaluated the RC building up to the collapse state, not near collapse state. Porter et al. also explain that the dataset's quality is high if the μ or β differences are found to be ≥ 20%.

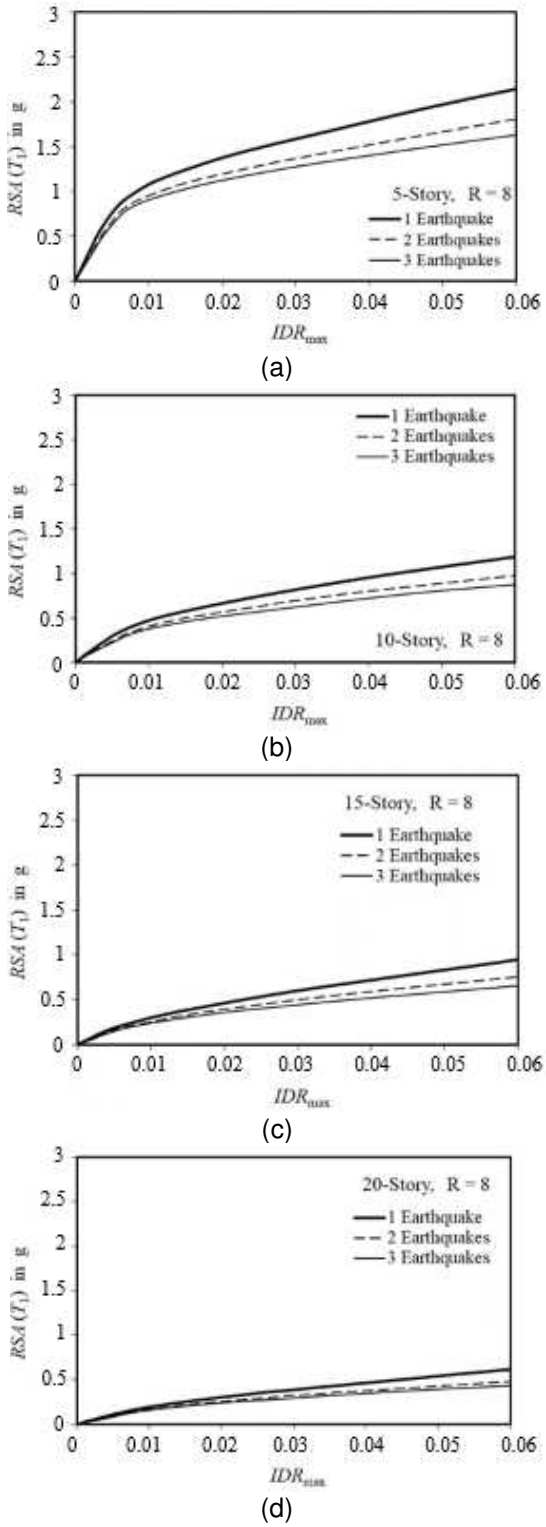

Figure 4. Average Maximum Inter-Story Drift Ratio of 5- to 20-Story SMF (R=8), Affected by Single Ground Motion (1GM) and Multiple Ground Motion (2GM and 3GM)

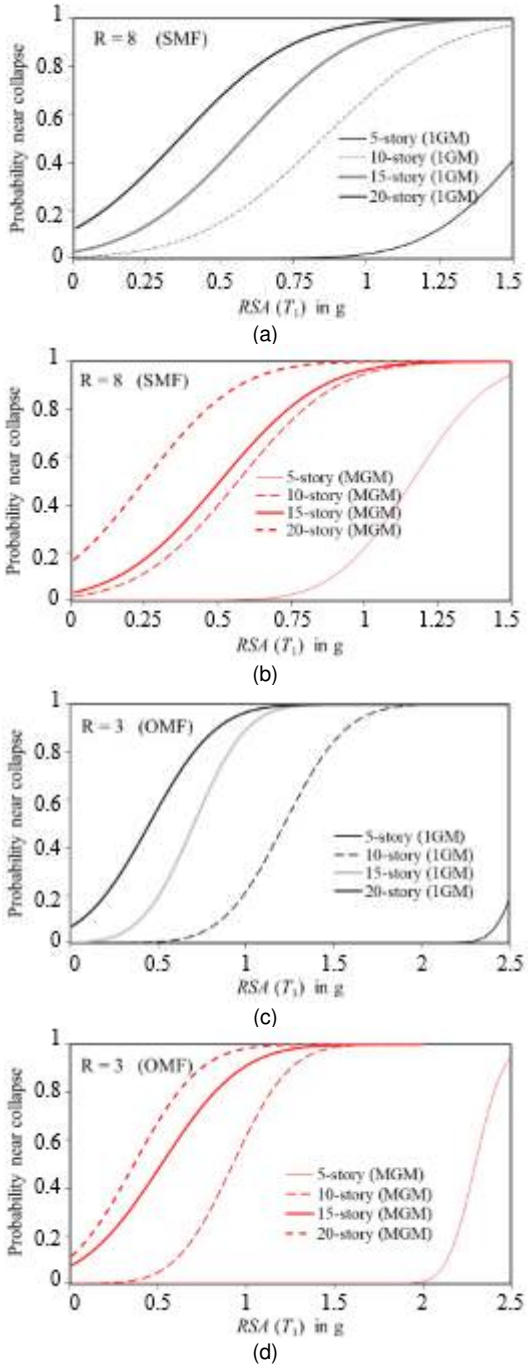

Figure 5. Probability of Near Collapse for 5-, 10-, 15-, and 20-Story SMF and OMF Induced by MGM with Fling-Step: a) 1GM Effect on the SMF, b) Maximum MGM Effect on the SMF, c) 1GM Effect on the OMF, d) Maximum MGM Effect on the OMF

This study found μ and β the difference was the same as indicated by Porter et al. Therefore, it can be concluded that the high quality of fragility functions in this study was well defined and calculated.

For all types considered MRF, the increase of *EDP* at elastic conditions caused by 2GM is reached 20.3% higher than the *EDP* caused by 1GM. This elastic condition is slightly different from *EDP* due to 3GM, 26.80% higher than the *EDP* response due to 1GM. The change in factor *R* is not visible at this condition, as indicated in Figure 4. The significance of the response of 2GM and 3GM is clearly detected when the magnitude of *IM* increased and arrived at the inelastic condition, which is posed at near- and after-line of near collapse *EDP*.

The 2GM has increased the response of 5-story OMF by 28.64% earlier than the *IM* of 1GM. This *IM* could be lower at 45.95% than the *IM* of

1GM when 3GM affect the OMF. In this post-elastic stiffness region, several of R's effect on the response appears, as indicated in the *IM* of 3GM when induced to the SMF. It has produced an *IM* of 89.11% lower than the *IM* of 1GM for near collapse *EDP*. This is almost two times larger than the *IM* for the *EDP* response of OMF.

The percentage of decrement *IM* for the near collapse EDP under the influence of multiple motions has showed not largely different under various story types (various fundamental periods). It is clearly indicated in 20- and 5-story *EDP* (Figure 5), which exhibited the *EDP* earlier with *IM* of 42.70% and 45.60% lower than *IM* of 2GM, respectively. These *IM* effects would more likely decrease up to 79.40% and 71.40% if 3GM induced SMF, respectively, compared with *IM* of 1GM.

The maximum response to the near collapse state caused by RE was exhibited on the 10-story MRF, which needed an *IM of* 86.90% lesser than the *IM of* 1GM. While the 20-story MRF experienced minimum response to near collapse state in this study when RE with *IM* of 32.50% lower than *IM* of 1GM induced to the frames. In general, it was found that all frames might pose the near collapse EDP early with *IM* lower of 45.15% and 68.37% than *IM* of 1GM, when 2GM and 3GM were induced to the frames, respectively.

For SMF, the 2GM and 3GM might cause the near collapse *EDP* reached early with *IM* of 41.40% and 76.80% lower than *IM* of 1GM, respectively. The 2GM and 3GM were made the near collapse EDP occurred more likely for the IMF. These were needed *IM* of about 61.40% and 85.70% lower than the *IM* of 1GM. A similar trend was also found for OMF under 2GM and 3GM, which was achieving near collapse EDP with *IM* of 32.60% and 42.60%, respectively, lower than *IM* of 1GM.

From probabilistic analysis, it was found that the median *IM* for near collapse *EDP* of single ground motion (1GM) was in the range of 1.56 to 0.36, which was meant that as the story of MRF increased, the median *IM* for near collapse *EDP* was decreased. The standard deviation of *IM*, which could skew the diagonal line of the fragility curve, was found within the range 0.29 – 0.33 randomly.

The effect of multiple ground motion (MGM), a maximum of two- or three-times ground motions, was depicted in Figure 5 compared to the effect of single ground motion (1GM). The figure clearly indicated that the *IM* of MGM has caused the SMF to exhibit near collapse earlier than the effect of 1GM on the SMF. The median of *IM* for MGM was within the range of 0.25 to 1.16, which was about 13.81 %, increasing the probability of near collapse of SMF. A similar trend was also found for *OMF* under the influence of MGM, compared with 1GM. However, the increment of probability was significantly larger than SMF. One of the *OMF* might be reaching 26.52% of *IM* of MGM, which was earlier than the effect of 1GM in achieving near collapse EDP. This result was slightly less than the influence of MGM on the *IMF*. Overall, the effect of MGM on the considered MRF in this study could cause the required IM of 12.61% lower than the required *IM* of 1GM.

CONCLUSION

The seismic performance evaluation of the moment-resisting frame (MRF) has been presented. The assessment was using the single, two times and three times multiple ground motions (MGM) with the displacement fling-step pulse. This type of pulse was not commonly incorporated in the motion records for seismic evaluation of MRF since the data available was scarce. Four archetype RC frames were considered, namely 5-, 10-, 15-, and 20-story with reduction factors R = 8, 5, and 3, which represent special (SMF), intermediate (IMF), and ordinary MRF (OMF). These R factors were affecting the strength capacity of beam-column elements of M_{max}/M_y =1.13 and the rotation capacity of 0.04 rad for SMF and 0.02 for IMF and OMF, which is based on experimental testing by others. The nonlinear inelastic response history analysis was conducted incrementally to develop the incremental dynamic analysis curve and calculate the median and standard deviation. Therefore, the following insight can be concluded:

1. On average, two- and three-times multiple ground motions (2GM and 3GM, respectively) have increased the engineering demand parameter (*EDP*), which was inter-story drift *IDR* in this study, up to 23.53% compared with the *EDP* caused by single ground motions (1GM). These 2GM and 3GM effects were measured under the same intensity measure ($IM = RSA(T_1)$) with the single earthquake (1GM) and were within the linear elastic condition. Therefore, the difference in *EDP* caused by 2GM and 3GM was found not significant.
2. The 2GM and 3GM have made *IM* shift more than half earlier than *IM* of 1GM in producing near collapse inter-story drift (*IDR = 2%*), which was selected near collapse EDP in this study. The 2GM has propagated the *IM* of near collapse shifted earlier than *IM* of 1GM for all MRF considered in the study. Both

might produce the *IM* of near collapse reached 68.37% lower than the *IM* of 1GM. Moreover, the 2GM and 3GM have caused special MRF to produce the near collapse EDP, with IM reaching 76.76% lower than the *IM* of 1GM. A similar trend was also found for intermediate and ordinary MRFs, which might be reached the *IM* of 85.71% and 42.64% earlier than the *IM* of 1GM, respectively.

3. The probabilistic analysis shows that the multiple ground motion's *IM* for near collapse *EDP* of SMF decreases compared to single ground motion. The probability of near collapse due to MGM is increased, either caused by 2GM or 3 GM, in comparison with 1GM. Similar findings were also demonstrated in the IMF and OMF under MGM. However, IMF produces a maximum response of MGM, compared with SMF and OMF
4. Indeed, the findings herewith might also be due to the variations in considered story heights, R = 3 to 8, and rotation capacity, which has also contributed to the critical effect on the seismic performance of the structure, besides the multiple ground motions containing filing-step pulse.

ACKNOWLEDGMENT

The internal grant supported by Universitas Muhammadiyah Sumatera Utara is greatly acknowledged. Furthermore, the author wishes to thank my undergraduate students involved in this research as the numerator.

REFERENCES

[1] T. A. Majid, H. W. Wan, S. S. Zaini, A. Faisal and Z. M. Wong, "The effect of ground motion on nonlinear performance of asymmetrical reinforced concrete frames," *Disaster Advances*, vol. 3, no. 4, pp.35-39, 2010.

[2] L. Dahal, H. Burton, and S. Onyambu, "Quantifying the effect of probability model misspecification in seismic collapse risk assessment," *Structural Safety*, vol. 96, ID: 102185, 2022, doi: 10.1016/j.strusafe. 2022.102185

[3] A. Rashidi, T. A. Majid, M. N. Fadzli, A. Faisal, and S. M. Noor," A comprehensive study on the influence of strength and stiffness eccentricities to the on-plan rotation of asymmetric structure," In *AIP Conference Proceedings,* vol. 1892, no. 1, p. 120013, 2017, doi: 10.1063/1.5005754

[4] V. Mohsenian, R. Filizadeh, I. Hajirasouliha, R. Garcia,"Seismic performance assessment of eccentrically braced steel frames with energy-absorbing links under sequential earthquakes," *Journal of Building Engineering*, vol. 33, ID: 101576, 2021, doi: 10.1016/j.jobe.2020.101576

[5] F. Di Trapani and M. Malavisi, "Seismic fragility assessment of infilled frames subject to mainshock/aftershock sequences using a double incremental dynamic analysis approach," *Bulletin of Earthquake Engineering*, vol. 17, no.1, pp. 211-235, 2019, doi: 10.1007/s10518-018-0445-2

[6] X. Guo, Z. He, and J. Xu, "Identification of incremental seismic damage development in RC structures excited with sequence-type ground motions," *Structures*, vol. 24, pp. 464-476, 2020, doi: 10.1016/j.istruc.2020. 01.012

[7] R. Oyguc, C. Toros, and A. E. Abdelnaby, "Seismic behavior of irregular reinforced-concrete structures under multiple earthquake excitations," *Soil Dynamics and Earthquake Engineering*, vol.104, pp. 15-32, 2018, doi: 10.1016/j.soildyn.2017.10.002

[8] L. Di Sarno and F. Pugliese, "Seismic fragility of existing RC buildings with corroded bars under earthquake sequences," *Soil Dynamics and Earthquake Engineering*, vol.134, pp.106169, 2020, doi: 10.1016/j.soildyn.2020.106169

[9] J. Ruiz-García, S. Yaghmaei-Sabegh and E. Bojórquez, "Three-dimensional response of steel moment-resisting buildings under seismic sequences," *Engineering Structures*, vol. 175, pp.399-414, 2018, doi: 10.1016/j.engstruct.2018.08.050

[10] S. D. Parekar and D. Datta, "Seismic behaviour of stiffness irregular steel frames under mainshock–aftershock," *Asian Journal of Civil Engineering*, vol. 21, no. 5, pp. 857-870, 2020, doi: 10.1007/s42107-020-00245-z

[11] L. Di Sarno, S. Amiri, and A. Garakaninezhad, "Effects of incident angles of earthquake sequences on seismic demands of structures," *Structures*, vol. 28, no. 1, pp. 1244-1251, 2020, doi: 10.1016/ j.istruc.2020.09.064

[12] A. Ayuddin, "Global structural analysis of high-rise hospital building using earthquake resistant design approach," *SINERGI*, vol. 24, no. 2, pp. 95-108, 2020, doi: 10.22441/sinergi.2020.2.003

[13] FEMA P-58-1 *Seismic Performance Assessment of Buildings, Volume 1 - Methodology*, 2nd Edition, Applied Technology Council, Redwood City, 2018

[14] FEMA (2018) FEMA P-58-2, *Seismic Performance Assessment of Buildings, Volume 2 – Implementation Guide,* 2nd

Edition, Applied Technology Council, Redwood City, 2018
[15] FEMA P-58-5, *Seismic Performance Assessment of Buildings, Volume 5 – Expected Seismic Performance of Code-Conforming Buildings,* 2nd Edition, Applied Technology Council, Redwood City, 2018.
[16] A. J. Carr, "*Ruaumoko Manual Volume: 1, Theory and User Guide to Associated Program,*" *Canterbury:* University of Canterbury, 2010.
[17] Badan Standarisasi Nasional, "*Tata Cara Perencanaan Ketahanan Gempa Untuk Struktur Bangunan Gedung dan Non Gedung SNI 1726:2012,"* Jakarta: Departemen Pekerjaan Umum, 2012.
[18] ASCE, *Minimum Design Loads for Buildings and Other Structures*, ASCE Standard ASCE/SEI 7-10, Reston: American Society of Civil Engineers, 2013.
[19] F. Ge, M. Tong, and Y. Zhao, "A structural demand model for seismic fragility analysis based on three-parameter lognormal distribution," *Soil Dynamics and Earthquake Engineering*, vol. 147, ID: 106770, 2021, doi: 10.1016/j.soildyn.2021.106770
[20] B. Huang, S. Günay & W. Lu, "Seismic Assessment of Freestanding Ceramic Vase with Shaking Table Testing and Performance-Based Earthquake Engineering," *Journal of Earthquake Engineering*, 2021, doi: 10.1080/13632469.2021.1979132
[21] F. Basone, L. Cavaleri, F. Di Trapani and G. Muscolino, "Incremental dynamic based fragility assessment of reinforced concrete structures: Stationary vs. non-stationary artificial ground motions," *Soil Dynamics and Earthquake Engineering*, vol. 103, pp. 105-117, 2017, doi: 10.1016/j.soildyn.2017.09.019
[22] M. Shokrabadi, H. V. Burton, and J. P. Stewart, "Impact of sequential ground motion pairing on mainshock-aftershock structural response and collapse performance assessment," *Journal of Structural Engineering*, vol. 144, no.10, 2018, doi: 10.1061/(asce)st.1943-541x.0002170

NOTATION LIST

β	= standard deviation
β_u	= logarithmic standard deviation
β_{IM}	= standard deviation of IM
$\mu_{\theta,c}$	= ductility of plastic rotation capacity
$\mu_{\theta,u}$	= ultimate rotation ductility
μ	= median
$\mu_{RSA(T_1)}$	= median of $RSA(T_1)$
θ_c	= plastic rotation capacity
θ_p	= plastic rotation capacity
θ_y	= yield rotation
θ_{pc}	= post-capping rotation capacity
ϕ	= standard lognormal cumulative distribution function
f_c'	= compressive strength
f_y	= yield strength
r	= bi-factor
EDP	= engineering demand parameter
$IDR_{\max}$	= maximum Inter-story drift ratio
IM	= intensity measure
$RSA(T_1)$	= spectrum response of acceleration at considered fundamental period as intensity measure
M_c / M_y	= ratio of capping moment and yield moment
$M_{\max}$	= maximum flexural strength
M_y	= yield flexural strength

ABBREVIATION LIST

GM	=	Ground motion
IDA	=	Incremental Dynamic Analysis
IMF	=	Intermediate Moment Resisting Frame
ISD	=	Incremental Seismic Damage
MRF	=	Moment Resisting Frame
OMF	=	Ordinary Moment Resisting Frame
PEER	=	Pacific Earthquake Engineering Research
NGA	=	Next Generation Attenuation
RC	=	Reinforced Concrete
RSA	=	Response Spectrum Acceleration
SMF	=	Special Moment Resisting Frame
SNI	=	Standar Nasional Indonesia (Indonesian Seismic Code)